2-3-2023

Endogenous L- to D-amino acid residue isomerization modulates selectivity between distinct neuropeptide receptor family members

Baba M. Yussif

Cole V. Blasing

James W. Checco

PNAS RESEARCH ARTICLE | BIOCHEMISTRY CHEMISTRY

Endogenous L- to D-amino acid residue isomerization modulates selectivity between distinct neuropeptide receptor family members

Baba M. Yussif[a], Cole V. Blasing[a], and James W. Checco[a,b,1]

Edited by Wilfred van der Donk, University of Illinois at Urbana-Champaign, Urbana, IL; received October 14, 2022; accepted February 3, 2023

The L- to D-amino acid residue isomerization of neuropeptides is an understudied post-translational modification found in animals across several phyla. Despite its physiological importance, little information is available regarding the impact of endogenous peptide isomerization on receptor recognition and activation. As a result, the full roles peptide isomerization play in biology are not well understood. Here, we identify that the *Aplysia* allatotropin-related peptide (ATRP) signaling system utilizes L- to D-residue isomerization of one amino acid residue in the neuropeptide ligand to modulate selectivity between two distinct G protein-coupled receptors (GPCRs). We first identified a novel receptor for ATRP that is selective for the D2-ATRP form, which bears a single D-phenylalanine residue at position 2. Using cell-based receptor activation experiments, we then characterized the stereoselectivity of the two known ATRP receptors for both endogenous ATRP diastereomers, as well as for homologous toxin peptides from a carnivorous predator. We found that the ATRP system displayed dual signaling through both the $G\alpha_q$ and $G\alpha_s$ pathways, and each receptor was selectively activated by one naturally occurring ligand diastereomer over the other. Overall, our results provide insights into an unexplored mechanism by which nature regulates intercellular communication. Given the challenges in detecting L- to D-residue isomerization from complex mixtures de novo and in identifying receptors for novel neuropeptides, it is likely that other neuropeptide-receptor systems may also utilize changes in stereochemistry to modulate receptor selectivity in a manner similar to that discovered here.

neuropeptide | isomerization | DAACP | GPCR | cell-cell signaling

Neuropeptides and peptide hormones play critical roles in cell-to-cell communication through sequence- and structure-specific interactions with receptor proteins. Cell-to-cell signaling peptides are among the largest class of transmitter molecules, which vary not only in terms of primary sequence but also a large number of functionally important post-translational modifications (PTMs). One relatively poorly understood peptide PTM is the enzyme-catalyzed isomerization of a ribosome-generated L-amino acid residue to its corresponding D-amino acid residue, which produces a D-amino acid-containing peptide (DAACP, Fig. 1) (1–3). Despite the subtlety of this modification, L- to D-residue isomerization can have a significant impact on the biological functions of DAACPs, including increased potency in physiological assays or altered kinetics of downstream responses (4–12). Functional DAACPs have been identified in diverse species across multiple phyla (including chordates, arthropods, and mollusks), and generally act as cell-to-cell signaling peptides (neuropeptides or peptide hormones) or as toxins (1, 2). However, DAACPs remain difficult to identify and characterize through routine endogenous peptide discovery efforts because L- to D-residue isomerization does not change the compound's mass or chemical composition. As a result, DAACPs remain relatively understudied as cell–cell signaling molecules, and undiscovered DAACPs are likely to exist across a variety of species.

Despite continuing advances in the detecting and identifying peptide isomers (13–18), relatively little is known about the functional impact of L- to D-residue isomerization in cell–cell signaling peptides on receptor recognition and activation. This lack of information is primarily due to a lack of identified receptors for endogenous cell–cell signaling DAACPs. To date, two receptors for endogenous cell–cell signaling DAACPs have been identified. The first is the achatin receptor, which is exclusively activated by the DAACP form of achatin-related peptides (19, 20). We recently discovered the second DAACP receptor, which belongs to the *Aplysia californica* allatotropin-related peptide (ATRP) signaling system (21). ATRP is a 14-residue amidated peptide that naturally exists as two diastereomers in the animal's central nervous system: all-L-ATRP and D2-ATRP, which contains a D-phenylalanine at position 2 (Fig. 1). In contrast to the achatin system, the recently

Significance

Neuropeptides are cell-to-cell signaling molecules that facilitate communication between neurons, and play important roles in physiology. Some neuropeptides undergo a post-translational modification in which an amino acid residue is converted from the L-stereoisomer to the D-stereoisomer. The impact of this change in peptide chirality is not well understood due to difficulties in identifying this modification and a lack of information regarding the receptor proteins for these neuropeptides. In this study, we discovered a neuropeptide signaling system in which naturally occurring amino acid isomerization in the neuropeptide ligand alters the selectivity between two distinct cell surface receptors. These results reveal a mechanism wherein nature utilizes a change in neuropeptide stereochemistry to modulate the signaling pathways activated.

Author contributions: J.W.C. designed research; B.M.Y., C.V.B., and J.W.C. performed research; B.M.Y. and J.W.C. analyzed data; and B.M.Y., C.V.B., and J.W.C. wrote the paper.

The authors declare no competing interest.

This article is a PNAS Direct Submission.

[1]To whom correspondence may be addressed. Email: checco@unl.edu.

This article contains supporting information online at https://www.pnas.org/lookup/suppl/doi:10.1073/pnas.2217604120/-/DCSupplemental.

Published March 6, 2023.

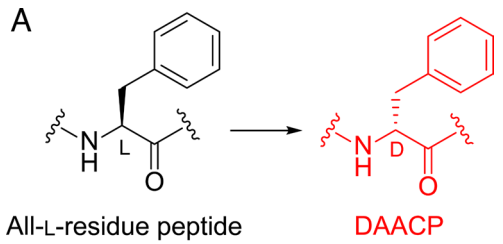

B

All-L-ATRP	GFRLNSASRVAHGY-NH_2
D2-ATRP	GfRLNSASRVAHGY-NH_2
ATRP(3-14)	RLNSASRVAHGY-NH_2
All-L-Conp	AFVKGSAQRVAHGY-NH_2
D2-Conp	AfVKGSAQRVAHGY-NH_2

Fig. 1. (*A*) Chemical structure showing the L- to D-amino acid residue isomerization of an all-L-residue peptide to form a DAACP. (*B*) Sequences of ATRP and Conp diastereomers examined in this study. D-residues are indicated by red lower-case letters.

discovered ATRP receptor (here called "ATRPR1") is activated by both peptide diastereomers, with all-L-ATRP being a significantly more potent agonist than D2-ATRP. The substantial deviation in receptor functionality for the achatin diastereomers versus the ATRP diastereomers demonstrates that the role of L- to D-residue isomerization in cell–cell signaling is highly complex. However, the relative lack of information regarding endogenous DAACP–receptor interactions impedes our understanding of this phenomenon.

Here we report the discovery and functional characterization of a novel receptor for *Aplysia* ATRPs, termed "ATRPR2." ATRPR2 represents only the third identified receptor for a cell–cell signaling DAACP to be functionally characterized, after the achatin receptor and ATRPR1. In stark contrast to ATRPR1, ATRPR2 was much more potently activated by D2-ATRP than all-L-ATRP. Thus, each ATRP diastereomer preferentially activates a different receptor target. To our knowledge, this is the first example of nature utilizing L- to D-residue isomerization in endogenous neuropeptides to modulate selectivity between distinct receptors. Taken together, our results reveal important insights into the regulation of cell–cell signaling through a subtle and understudied PTM.

Results

Discovery and Cloning of ATRPR2. During the discovery and characterization of ATRPR1 (21), we noticed that the *Aplysia* transcriptome contained transcripts encoding several additional ATRPR-like proteins. Based on this observation, we hypothesized that some of these proteins may be additional receptors for ATRP ligands. To test this hypothesis, we began the present study by performing tBLASTn searches of the NCBI *Aplysia californica* transcriptome shotgun assembly (22) and the transcriptome assemblies available through the *Aplysia* Gene Tools database (http://aplysiatools.org/) (23–26) using ATRPR1 (XP_005106214.1) as the query. Among the top hits from these searches was an mRNA transcript with translated protein sequence predicted to be a full-length GPCR (*SI Appendix*, Fig. S1), and that aligned well with ATRPR1 (*SI Appendix*, Fig. S2). This protein is a putative ATRP receptor, which we call ATRPR2. ATRPR2 was then cloned into a pcDNA3.1(+) vector for expression in mammalian cells.

Activation of the Gα_q Pathway by ATRPRs. To determine whether ATRPR2 is a receptor for ATRPs, ATRPR2 in pcDNA3.1(+) was transiently transfected into CHO-K1 cells to facilitate receptor expression on the cell surface, and the cells were then treated with all-L-ATRP or D2-ATRP. Because ATRPR1 was previously shown to signal through the Gα_q signaling pathway (21), we evaluated the ability of all-L-ATRP or D2-ATRP to activate ATRPRs via this pathway by monitoring the accumulation of D-*myo*-inositol 1-monophosphate (IP1), a product of phospholipase C activation characteristic of Gα_q family signaling (27) (Fig. 2 and *SI Appendix*, Figs. S3–S6). Consistent with our previous report (21), we found that ATRPR1 was activated by both all-L-ATRP and D2-ATRP, with all-L-ATRP being a more potent agonist at this receptor. We found that ATRPR2 was also activated by both diastereomers, consistent with our hypothesis that ATRPR2 was a receptor for ATRP ligands. However, in contrast to ATRPR1, ATRPR2 was much more potently activated by D2-ATRP (EC_{50} = 2 nM) than by all-L-ATRP (EC_{50} = 400 nM). A truncated analog of ATRP lacking the two N-terminal residues, ATRP (3-14) (Fig. 1), had very low potency for ATRPR2 (EC_{50} = 10,000 nM), indicating that the N-terminal Gly and L/D-Phe residues are critical for potent receptor activation.

In addition to evaluating activation by ATRPs, we also examined whether ATRPR2 could be activated by all-L-Conp and D2-Conp (Fig. 1), diastereomeric peptides found in the venom of the cone snail *Conus vitulinus* (28). Given their high sequence similarity to allatotropins, it is hypothesized that these Conp peptides act on allatotropin receptors found within the prey of the cone snail. Interestingly, D2-Conp was a highly potent agonist of ATRPR2, with a potency (EC_{50} = 2 nM) matching that of D2-ATRP. All-L-Conp was a much weaker agonist, with potency (EC_{50} = 300 nM) similar to that of all-L-ATRP. This result contrasts with the activity of Conp peptides at ATRPR1 (21), in which both diastereomers were demonstrated to be relatively weak agonists. This result may suggest that D2-Conp, which is the major diastereomer of the peptide found in the cone snail venom (28), likely targets receptors more similar to ATRPR2 than ATRPR1 during predation or defense.

Activation of the Ga_s Pathway by ATRPRs. In addition to activating the Gα_q pathway, allatotropin receptors in insects have previously been shown to increase intracellular cyclic adenosine monophosphate (cAMP) concentration, suggesting they may also activate the Gα_s pathway (29–33). Mammalian orexin receptors, which are evolutionarily related to allatotropin receptors (34, 35), have also been shown to signal through several G protein-mediated pathways simultaneously (36). To determine whether this interesting dual signaling also occurs for the *Aplysia* ATRPRs, we measured cAMP accumulation in CHO-K1 cells in response to peptide ligand stimulation for each receptor (Fig. 3 and *SI Appendix*, Figs. S7–S10). For both ATRPR1 and ATRPR2, stimulation by ATRPs led to an increase in intracellular cAMP, suggesting that both of these receptors are able to couple to Gα_s family proteins endogenous to the CHO-K1 cells. In cAMP experiments, we found that ATRPR1 was more selective for all-L-ATRP (EC_{50} = 10 nM) over D2-ATRP (EC_{50} = 800 nM). In contrast, ATRPR2 was more selective for D2-ATRP (EC_{50} = 5 nM) over all-L-ATRP (EC_{50} = 3,000 nM) in cAMP assays. These results in cAMP assays mirror the selectivity observed in the IP1 assays for these two receptors. Interestingly, the receptor selectivity appears to be somewhat more pronounced for cAMP response relative to IP1 response for both receptors. For ATRPR1, all-L-ATRP was found to be ~20-fold more potent than D2-ATRP in IP1 experiments, but ~80-fold more potent than D2-ATRP in cAMP experiments. Similarly, for

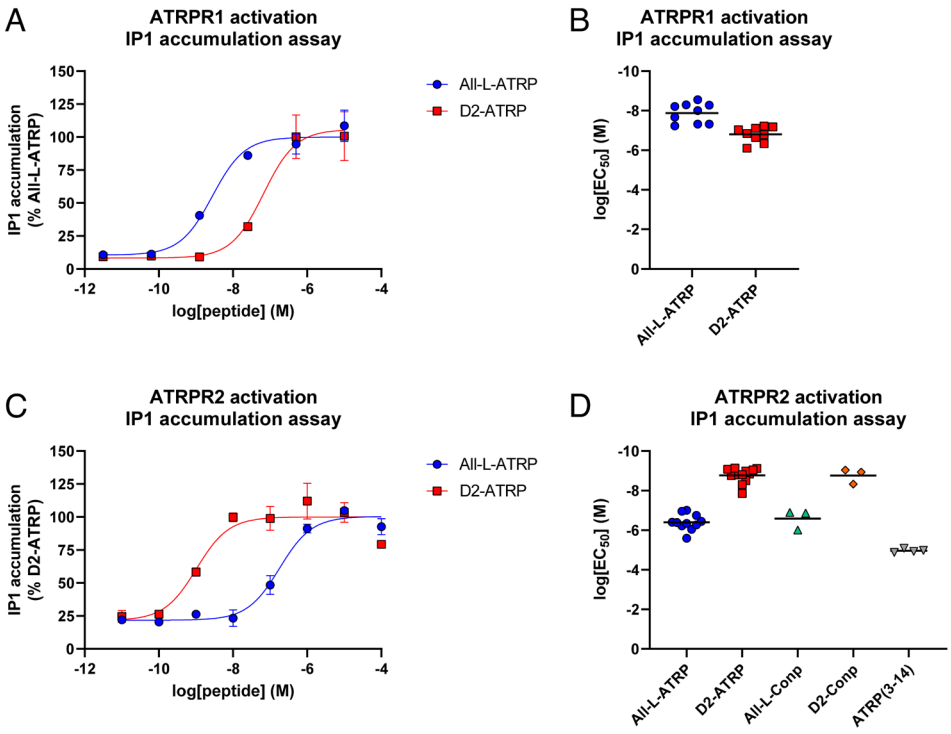

E

Peptide	ATRPR1 (IP1) log[EC₅₀] (M)	ATRPR1 (IP1) EC₅₀ (nM)	ATRPR2 (IP1) log[EC₅₀] (M)	ATRPR2 (IP1) EC₅₀ (nM)
All-L-ATRP	-7.9 ± 0.5	10	-6.4 ± 0.4	400
D2-ATRP	-6.8 ± 0.4	200	-8.8 ± 0.4	2
All-L-Conp	ND	ND	-6.6 ± 0.5	300
D2-Conp	ND	ND	-8.8 ± 0.4	2
ATRP(3-14)	ND	ND	-5.0 ± 0.1	10,000

Fig. 2. Activation of ATRPR1 and ATRPR2 through the $G\alpha_q$ signaling pathway, as measured by IP1 accumulation assay in transiently transfected CHO-K1 cells. (*A*) Representative experiment showing dose–response curves for ATRPR1. Each point represents the mean ± SD of duplicate wells on the plate. (*B*) Graphical summary of all experiments used to calculate mean log[EC_{50}] values for ATRPR1. Each point represents the log[EC_{50}] value from an independent experiment, and each horizontal line indicates the mean for that peptide. See *SI Appendix*, Fig. S5 for statistical comparisons. (*C*) Representative experiment showing dose–response curves for ATRPR2. Each point represents the mean ± SD of duplicate wells on the plate. (*D*) Graphical summary of all experiments used to calculate mean log[EC_{50}] values for ATRPR2. Each point represents the log[EC_{50}] value from an independent experiment, and each horizontal line indicates the mean for that peptide. See *SI Appendix*, Fig. S5 for statistical comparisons. (*E*) Potency values for peptides tested at each receptor. Log[EC_{50}] values are reported as the mean ± SD from at least three independent experiments. Linear EC_{50} values are rounded to 1 significant figure. ND = not determined.

ATRPR2, D2-ATRP was found to be ~200-fold more potent than all-L-ATRP in IP1 experiments, but ~600-fold more potent than all-L-ATRP in cAMP experiments.

We also evaluated the ability of all-L-Conp and D2-Conp to activate ATRPRs in cAMP experiments. Consistent with the IP1 experiments, we found that D2-Conp was a potent agonist of ATRPR2 with an EC_{50} value similar to that of D2-ATRP (EC_{50} = 6 nM for D2-Conp), while all-L-Conp was a weak agonist of ATRPR2 (EC_{50} = 3,000 nM). Together, both the IP1 and cAMP accumulation data indicate that the toxin peptide D2-Conp is a highly potent agonist of ATRPR2.

Discussion

As a result of this study, the *Aplysia* ATRP signaling system is now known to consist of two diastereomeric peptides and (at least) two receptors: ATRPR1 and ATRPR2 (Fig. 4). Our results demonstrate that ATRPR2 has high selectivity for D2-ATRP, while ATRPR1 is more selective for all-L-ATRP. The ATRP signaling system contrasts distinctly with the only other DAACP signaling system studied at the receptor level (the achatin family), in which only the DAACP form is functional at identified receptors and in physiological measurements (11, 19, 20). As more receptors for DAACPs are identified, it will be important to determine whether other systems utilize L- to D-residue isomerization as an "on/off switch" (as in the achatin system) or to modulate selectivity at multiple receptors (as in the ATRP system). It is likely that isomerization-mediated changes in receptor selectivity are present in other DAACP families whose receptors have not yet been identified. For example, the distinct physiological responses elicited by the two naturally occurring diastereomers of crustacean hyperglycemic hormone (CHH) (6, 7) may be due to two or more CHH receptors with different preferences for the diastereomers.

The two diastereomers of ATRP are homologous to two naturally occurring diastereomeric peptides found in *Conus* venom, all-L-Conp and D2-Conp (28). In fact, it is this homology that initially led to the discovery that ATRP peptides exist as two diastereomers (21). *Conus* venom is comprised of a diverse array of peptides, which include the well-studied disulfide-rich conotoxins in addition to hormone-like peptides such as Conp (37). Conp

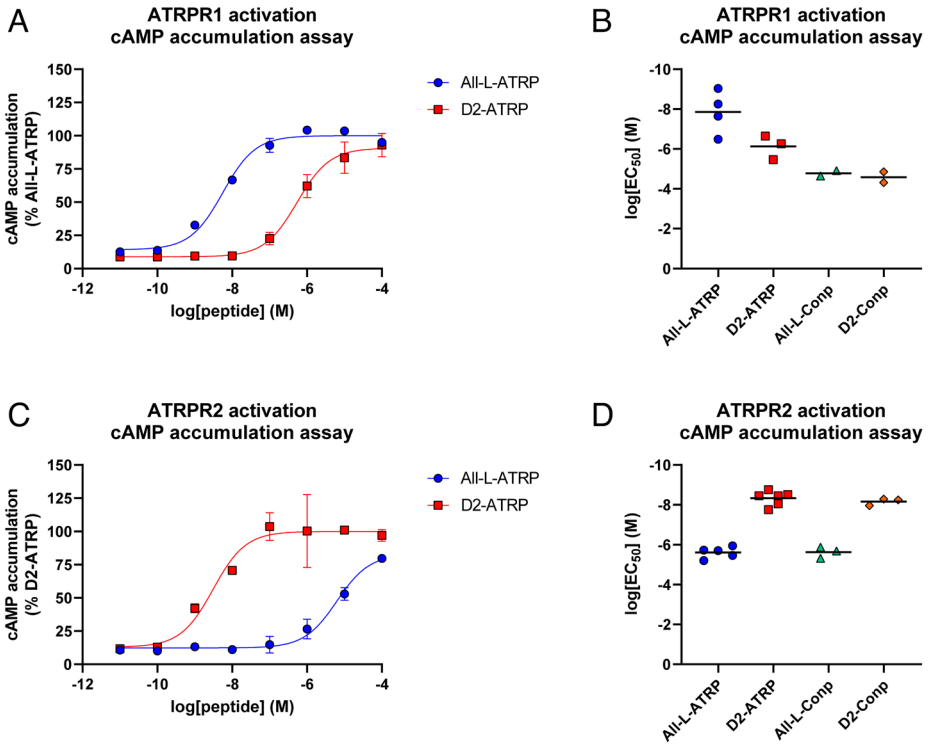

E

	ATRPR1 (cAMP)		ATRPR2 (cAMP)	
Peptide	log[EC₅₀] (M)	EC₅₀ (nM)	log[EC₅₀] (M)	EC₅₀ (nM)
All-L-ATRP	-7.9 ± 1.1	10	-5.6 ± 0.3	3000
D2-ATRP	-6.1 ± 0.6	800	-8.3 ± 0.4	5
All-L-Conp	-4.8 ± 0.2	20,000	-5.6 ± 0.3	3000
D2-Conp	-4.6 ± 0.4	30,000	-8.2 ± 0.2	6

Fig. 3. Activation of ATRPR1 and ATRPR2 through the $G\alpha_s$ signaling pathway, as measured by cAMP accumulation assay in transiently transfected CHO-K1 cells. (*A*) Representative experiment showing dose-response curves for ATRPR1. Each point represents the mean ± SD of duplicate wells on the plate. (*B*) Graphical summary of all experiments used to calculate mean log[EC_{50}] values for ATRPR1. Each point represents the log[EC_{50}] value from an independent experiment, and each horizontal line indicates the mean for that peptide. See *SI Appendix*, Fig. S9 for statistical comparisons. (*C*) Representative experiment showing dose–response curves for ATRPR2. Each point represents the mean ± SD of duplicate wells on the plate. (*D*) Graphical summary of all experiments used to calculate mean log[EC_{50}] values for ATRPR2. Each point represents the log[EC_{50}] value from an independent experiment, and each horizontal line indicates the mean for that peptide. See *SI Appendix*, Fig. S9 for statistical comparisons. (*E*) Potency values for peptides tested at each receptor. Log[EC_{50}] values are reported as the mean ± SD from at least two independent experiments. Linear EC_{50} values are rounded to 1 significant figure.

peptides belong to a relatively recently discovered family of conopeptides ("New Superfamily 1"), which appears to be a major component of the animal's defensive venom (38). Prior studies have demonstrated that Conp peptides exhibit contractile activity on mollusk muscle (28) and modulate excitability of mollusk neurons (21), but do not show similar activity on rat muscle (28). These results are consistent with a mode of action in which Conp peptides act through allatotropin-related peptide receptors, which are present across protostomes but have diverged into orexin receptors in vertebrates (34, 35). The widespread abundance of allatotropin-related receptors across diverse organisms may help explain why Conp-related peptides are present as a component in cone snail venom. We have shown that both diastereomers of Conp are weak-to-moderate agonists for ATRPR1, while D2-Conp is a potent agonist of ATRPR2. It is possible that *Conus* evolved L- to D-residue isomerization in Conp peptides as a means to target ATRPR2-like receptors in prey. Alternatively, it is possible that these animals utilize isomerization in their own cell–cell signaling peptides, which were then co-opted into the venom (37).

There are several unanswered questions that remain exciting directions for future research. First, in addition to ATRPR2, we also attempted to clone and functionally evaluate several additional putative *Aplysia* ATRPRs identified from BLAST searches, but none of these other receptors proved to be functional receptors for ATRPs. This may be due to a number of factors, including incomplete or incorrect sequences deposited in the database or deficiencies in functional expression on the CHO-K1 cells. Nevertheless, the existence of additional receptors with high similarity to ATRPR1 and ATRPR2 in the *Aplysia* transcriptome raises the possibility that more receptors may exist. Second, we observed that both ATRPR1 and ATRPR2 displayed higher diastereomeric selectivity in cAMP assays relative to IP1 assays. This result suggests that for a given receptor, each ligand may differ in their ability to activate intracellular pathways, representing an endogenous example of functional selectivity/ligand bias (39–41) modulated by L- to D-residue isomerization. Finally, the presence of a D-residue near the peptide's N terminus provides increased stability to aminopeptidases (14). Because *Aplysia* neuronal membranes and hemolymph are rich in aminopeptidases (42–45), D2-ATRP is predicted to have a longer biological half-life in the animal than all-L-ATRP. Indeed, in vitro stability studies demonstrated that D2-ATRP was significantly more stable in *Aplysia* hemolymph plasma than all-L-ATRP (21). The possibility that

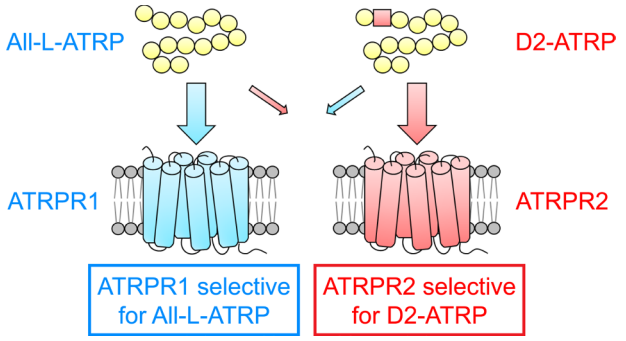

Fig. 4. The current model for peptide–receptor signaling in the *Aplysia* ATRP family.

D2-ATRP may have significantly longer biological lifetime in vivo adds a further layer of regulation for cell-to-cell signaling in this system. It will be of great interest to explore all of these areas in the future.

Progress in fully understanding the biological impact of L- to D-residue isomerization is hindered by three major challenges. First, peptide stereochemistry is not routinely evaluated in peptide characterization (i.e., "peptidomics") approaches and cannot be predicted based on genome or transcriptome (1, 2). Although there has been excellent recent progress in developing tools to identify DAACPs (13–18), there are likely many more DAACPs in nature than those currently identified. Second, relatively little is known about the L-/D-isomerases responsible for DAACP biosynthesis (1). Although several reports have studied chromatographic fractions containing isomerase activity (5, 46–48) and the sequences of two isomerases have been proposed (49, 50), the relative lack of information on these enzymes has slowed progress in characterizing DAACP signaling across animals. Third, identifying the receptors for bioactive peptides remains a significant challenge (51, 52). In this case, we were able to identify the putative ATRP receptors based on homology to known allatotropin receptors. However, many identified DAACPs do not benefit from such homology. Advancements in combinatorial screening (19), computational prediction (53, 54), transcriptome analysis (55, 56), and ligand–receptor capture (57, 58) continue to identify receptors for bioactive peptides, but DAACPs are not often included in such studies. As a result of these challenges, very few DAACP receptors are known (19–21). The results of this study shed important light onto how animals can utilize L- to D-residue isomerization in peptide ligands to modulate cell-to-cell communication through altering receptor selectivity. Given the understudied nature of this PTM and its occurrence across phyla (1, 2), it is likely that epimerization is used as a form of regulation in other peptide-receptor systems and is not restricted to *Aplysia* or to the ATRP family.

Materials and Methods

General. Unless otherwise specified, solvents and reagents were purchased from ThermoFisher Scientific or MilliporeSigma.

Peptide Synthesis. Peptides were synthesized by Fmoc solid-phase peptide synthesis (59) on NovaPEG rink amide resin (Novabiochem, 855047). Fmoc-protected amino acids were purchased from Novabiochem, Chem-Impex, AnaSpec, AstaTech, or AAPPTec. Each coupling solution contained four equivalents of protected amino acid, four equivalents of benzotriazole-1-yl-oxy-tris-pyrrolidino-phosphonium hexafluorophosphate (PyBOP), and eight equivalents of N,N-diisopropylethylamine, dissolved in N,N-dimethylformamide (DMF). Coupling reactions were carried out for 30 min to 24 h at room temperature, followed by rinsing the resin with DMF. Fmoc deprotection reactions were carried out using 20% piperidine in DMF for 10 to 15 min at room temperature, followed by rinsing the resin with DMF. Once the final amino acid in the sequence was coupled and the Fmoc group deprotected, the peptide was cleaved from the resin for a duration of 3 h using 95% trifluoracetic acid, 2.5% H_2O, and 2.5% triisopropylsilane. The cleaved peptides were precipitated with 40 mL of cold diethyl ether, then centrifuged (3,000 × g, 10 min) to form a peptide pellet. The diethyl ether was decanted, and the pellet was allowed to dry. The peptide pellet was then resuspended in 50% acetonitrile in H_2O and purified using reverse-phase high-performance liquid chromatography (HPLC). Matrix-assisted laser desorption/ionization Fourier transform ion cyclotron resonance mass spectrometry was used to confirm the peptide identity, while peptide purity was evaluated via analytical-scale HPLC (*SI Appendix*, Fig. S11).

Receptor Cloning. A synthetic gene block containing the sequence for the ATRPR2-encoding transcript (*SI Appendix*, Fig. S1) and appropriate primers were purchased from Integrated DNA technologies. To facilitate expression in mammalian cells, the ATRPR2 open reading frame (ORF) was cloned into pcDNA3.1(+) (ThermoFisher Scientific, V79020). Briefly, Q5 Hot Start Polymerase (New England Biolabs, M04935) was used to perform a PCR of the predicted ORF from the gene block using the following primers: forward 5′-ATAAAGCTTGTTGTTGTGCAGTCTTTGAG-3′, reverse 5′-ATACTCGAGTCATGCGGTACATTGTATTC-3′. The PCR was performed at the following thermal cycling conditions: initial denaturation at 98 °C for 30 s; 30 cycles of denature at 98 °C for 10 s, anneal at 68 °C for 30 s, extend at 72 °C for 1 min; final extension at 72 °C for 2 min. The forward primer consists of a HindIII restriction enzyme cut site and the reverse primer consists of an XhoI restriction enzyme cut site. The resulting PCR amplicon and empty pcDNA3.1(+) plasmid were each double digested with HindIII and XhoI restriction enzymes (ThermoFisher Scientific, K1991) at the following conditions: incubation at 37 °C for 60 min; thermal inactivation at 80 °C for 15 min. The bands corresponding to digested receptor amplicon and plasmid were each purified from a 1% agarose gel using a DNA clean and concentrator kit (Zymo Research, D4004) with agarose dissolving buffer (Zymo Research, D4001-1-100). The restriction enzyme-digested insert containing the ATRPR2 sequence was ligated to the restriction enzyme-digested pcDNA3.1(+) vector using T4 DNA ligase (New England Biolabs, M0202S) in a 20 μL ligation reaction at room temperature for 2 h, followed by thermal inactivation at 65 °C for 10 min. The ligation product (5 μL) was then transformed into a 50 μL suspension of chemically competent *Escherichia coli* (DH5α) cells (ThermoFisher Scientific, 18265017) by heat shock (30 min on ice, then 30 s at 42 °C, then 2 min on ice). S.O.C. medium (200 μL, ThermoFisher Scientific, 15544034) was then added to the cells and incubated at 37 °C for 30 min to allow the cells to recover, after which the cells were plated on Luria–Bertani (LB) agar plates supplemented with 100 μg/mL ampicillin and incubated overnight at 37 °C. A single colony from the plate was cultured in 200 mL of LB with 100 μg/mL ampicillin and incubated overnight at 37 °C while shaking. The plasmid was purified using Omega Bio-TEK E.Z.N.A plasmid DNA Maxi kit (D6922-02), following the manufacturer's instructions. Correct incorporation of the ORF into plasmid was confirmed by DNA sequencing (Eurofins Genomics).

Cell Culture. CHO-K1 cells (ATCC, CCL-61) were cultured at 37 °C, 5% CO_2 in Ham's F-12K (Kaighn's) medium (ThermoFisher Scientific, 21127022) supplemented with 10% fetal bovine serum (FBS) (VWR, 97068-085); 1× PenStrep solution (Fisher, SV30010; final concentration penicillin = 100 U/mL, streptomycin = 100 μg/mL). Cells were maintained in T75 cell culture plates and passaged regularly to avoid over-confluence. In advance of a GPCR activation experiment (Day 1), cells were detached from the plate using 0.05% trypsin-ethylenediaminetetraacetic acid (EDTA) (Fisher Scientific, MT25052CI), and subcultured into a 35-mm-diameter tissue culture dish (Fisher Scientific, FB012920), and incubated overnight at 37 °C, 5% CO_2.

The next day (Day 2), when the cells reached 85 to 100% confluence, the medium was replaced with F-12K medium supplemented with 10% FBS and no antibiotics. Prior to transfection, 2 μg of receptor plasmid was mixed with 6 μL of Turbofect Transfection Reagent (ThermoFisher Scientific, R0531) in 200 μL of Opti-MEM Reduced Serum Medium (ThermoFisher Scientific, 31985070), and incubated at room temperature for 15 min. After this incubation, the plasmid/Turbofect mixture was added dropwise to the dish containing cells, and the cells were incubated at 37 °C, 5% CO_2 overnight. The next day (Day 3), the transfected cells were detached using 0.05% trypsin-EDTA and reseeded into white 96-well

half-area tissue culture-treated plates (Fisher Scientific, 07-200-309) in F-12K medium with 10% FBS and allowed to recover overnight at 37 °C, 5% CO_2. For IP1 accumulation assays, cells were plated at a density of 20,000 cells per well. For cAMP accumulation assays, cells were plated at a density of 5,000 cells per well. The next day (Day 4), activation of the receptor was evaluated using either IP1 accumulation assay or cAMP accumulation assay, as described below.

IP1 Accumulation Assays. IP1 accumulation was evaluated using an IPOne–Gq kit (Cisbio, 62IPAPEC) (27, 60). Serial dilutions of the peptides of interest were prepared in stimulation buffer (provided with the kit). From the 96-well half-area plates containing transfected cells, the cell culture medium was removed from each well and replaced with 14 μL of stimulation buffer, followed by 14 μL of the appropriate peptide dilution in stimulation buffer. The plate was then incubated at 37 °C, 5% CO_2 for ~1 to 2 h. The plate was then removed from the incubator. To generate an IP1 standard curve, serial dilutions of IP1 standard (28 μL, 11,000 nM to 2.7 nM) in stimulation buffer were added to empty wells on the plate. Next, 6 μL of 0.5× IP1-d2 and 6 μL of 0.5× anti-IP1-cryptate (provided with the kit) dissolved in lysis buffer (provided with the kit) were added to each working well and then incubated at room temperature on a rocker for 45 to 60 min. After incubation, homogeneous time-resolved fluorescence was read via a Biotek Synergy Neo2 plate reader using the following parameters: time-resolved fluorescence, delay: 150 μs, collection time: 500 μs; light source: xenon flash, lamp energy: high, dynamic range: extended, read speed: normal, read delay: 1 ms, measurements/data point: 50, read height: 5 mm. Filter set 1; Optics = Top, Gain = extended, excitation = 330/80 nm, emission = 665/8 nm. Filter set 2; Optics = Top, Gain = extended, excitation = 330/80 nm, emission = 620/10 nm. The 665 nm/620 nm ratio of fluorescence intensities for the standard wells was fitted to a four-parameter sigmoidal dose–response model in GraphPad Prism 9 to generate an IP1 standard curve. The resulting IP1 standard curve was used to calculate the IP1 concentration in each experimental well based on the measured 665 nm/620 nm ratio (60), and IP1 signal was normalized to the maximum response for a reference agonist within a given experiment (all-L-ATRP for ATRPR1 or D2-ATRP for ATRPR2). The IP1 accumulation data were fit to a three-parameter sigmoidal dose–response model in GraphPad Prism 9 to calculate log[EC_{50}] values. Experiments with average intra-assay coefficient of variation between technical replicates of <25% were used to calculate mean log[EC_{50}] and SD for independent experiments. Statistical analysis was performed using GraphPad Prism 9.

cAMP Accumulation Assays. cAMP accumulation was measured using cAMP–Gs HiRange kit (Cisbio, 62AM6PEC). Serial dilutions of the peptide were prepared in stimulation buffer (provided with the kit) supplemented with 500 μM 3-isobutyl-1-methylxanthine (IBMX) (AdipoGen, AG-CR1-3512) with 0.1% dimethyl sulfoxide (DMSO). From the 96-well plate containing transfected cells, the cell culture medium was removed from each well and replaced with 10 μL stimulation buffer, 500 μM IBMX, 0.1% DMSO, followed by 10 μL of the appropriate peptide dilution. The plate was then incubated at 37 °C, 5% CO_2 for ~1 to 2 h. The plate was then removed from the incubator. To generate a cAMP standard curve, serial dilutions of cAMP standard (20 μL, 14,000 nM to 0.34 nM) in stimulation buffer, 500 μM IBMX, 0.1% DMSO were added to empty wells on the plate. Next, 10 μL of 1× cAMP-d2 and 10 μL of 1× anti-cAMP-cryptate (provided with the kit) dissolved in lysis buffer (provided with the kit) were added to each well, and the plate was then incubated at room temperature on a rocker for 45 to 60 min. After incubation, homogeneous time-resolved fluorescence was read using a Biotek Synergy Neo2 plate reader, as described above. Data were fit and log[EC_{50}] values calculated using the same procedure described above for IP1 accumulation assays. Experiments with average intra-assay coefficient of variation between technical replicates of <25% were used to calculate mean log[EC_{50}] and SD for independent experiments. Statistical analysis was performed using GraphPad Prism 9.

Data, Materials, and Software Availability. All study data are included in the article and/or *SI Appendix*.

ACKNOWLEDGMENTS. This research was supported in part by the Nebraska Center for Integrated Biomolecular Communication (NCIBC, National Institute of General Medical Sciences P20 GM113126). C.V.B. was supported in part by a Undergraduate Creative Activities and Research Experience Award. We thank the Nebraska Center for Mass Spectrometry, NCIBC Systems Biology Core Facility, and the Research Instrumentation Facility for providing instrument access.

Author affiliations: [a]Department of Chemistry, University of Nebraska-Lincoln, Lincoln, NE 68588; and [b]The Nebraska Center for Integrated Biomolecular Communication, University of Nebraska-Lincoln, Lincoln, NE 68588

1. D. H. Mast, J. W. Checco, J. V. Sweedler, Advancing D-amino acid-containing peptide discovery in the metazoan. *Biochim. Biophys. Acta. Proteins Proteom.* **1869**, 140553 (2021).
2. C. Ollivaux, D. Soyez, J. Y. Toullec, Biogenesis of D-amino acid containing peptides/proteins: Where, when and how? *J. Pept. Sci.* **20**, 595–612 (2014).
3. K. Richter, R. Egger, G. Kreil, D-Alanine in the frog skin peptide dermorphin is derived from L-alanine in the precursor. *Science* **238**, 200–202 (1987).
4. M. Broccardo *et al.*, Pharmacological data on dermorphins, a new class of potent opioid peptides from amphibian skin. *Br. J. Pharmacol.* **73**, 625–631 (1981).
5. S. D. Heck *et al.*, Functional consequences of posttranslational isomerization of Ser46 in a calcium channel toxin. *Science* **266**, 1065–1068 (1994).
6. D. Soyez *et al.*, Evidence for a conformational polymorphism of invertebrate neurohormones. D-amino acid residue in crustacean hyperglycemic peptides. *J. Biol. Chem.* **269**, 18295–18298 (1994).
7. A. Yasuda, Y. Yasuda, T. Fujita, Y. Naya, Characterization of crustacean hyperglycemic hormone from the crayfish (*Procambarus clarkii*): Multiplicity of molecular forms by stereoinversion and diverse functions. *Gen. Comp. Endocrinol.* **95**, 387–398 (1994).
8. F. Morishita *et al.*, A novel D-amino-acid-containing peptide isolated from *Aplysia* heart. *Biochem. Biophys. Res. Commun.* **240**, 354–358 (1997).
9. E. Iwakoshi, M. Hisada, H. Minakata, Cardioactive peptides isolated from the brain of a Japanese octopus, *Octopus minor*. *Peptides* **21**, 623–630 (2000).
10. C. Ollivaux, D. Gallois, M. Amiche, M. Boscameric, D. Soyez, Molecular and cellular specificity of post-translational aminoacyl isomerization in the crustacean hyperglycaemic hormone family. *FEBS J.* **276**, 4790–4802 (2009).
11. L. Bai *et al.*, Characterization of GdFFD, a D-amino acid-containing neuropeptide that functions as an extrinsic modulator of the *Aplysia* feeding circuit. *J. Biol. Chem.* **288**, 32837–32851 (2013).
12. C. Y. Yang *et al.*, *Aplysia* locomotion: Network and behavioral actions of GdFFD, a D-amino acid-containing neuropeptide. *PLoS One* **11**, e0147335 (2016).
13. C. Jia, C. B. Lietz, Q. Yu, L. Li, Site-specific characterization of D-amino acid containing peptide epimers by ion mobility spectrometry. *Anal. Chem.* **86**, 2972–2981 (2014).
14. I. Livnat *et al.*, A D-amino acid-containing neuropeptide discovery funnel. *Anal. Chem.* **88**, 11868–11876 (2016).
15. D. H. Mast, J. W. Checco, J. V. Sweedler, Differential post-translational amino acid isomerization found among neuropeptides in *Aplysia californica*. *ACS Chem. Biol.* **15**, 272–281 (2019).
16. Y. Tao, R. R. Julian, Identification of amino acid epimerization and isomerization in crystallin proteins by tandem LC-MS. *Anal. Chem.* **86**, 9733–9741 (2014).
17. Y. Tao, N. R. Quebbemann, R. R. Julian, Discriminating D-amino acid-containing peptide epimers by radical-directed dissociation mass spectrometry. *Anal. Chem.* **84**, 6814–6820 (2012).
18. T. R. Lambeth *et al.*, Spontaneous isomerization of long-lived proteins provides a molecular mechanism for the lysosomal failure observed in Alzheimer's disease. *ACS Cent. Sci.* **5**, 1387–1395 (2019).
19. P. Bauknecht, G. Jékely, Large-scale combinatorial deorphanization of *Platynereis* neuropeptide GPCRs. *Cell Rep.* **12**, 684–693 (2015).
20. J. W. Checco *et al.*, Molecular and physiological characterization of a receptor for D-amino acid-containing neuropeptides. *ACS Chem. Biol.* **13**, 1343–1352 (2018).
21. J. W. Checco *et al.*, *Aplysia* allatotropin-related peptide and its newly identified D-amino acid-containing epimer both activate a receptor and a neuronal target. *J. Biol. Chem.* **293**, 16862–16873 (2018).
22. E. W. Sayers *et al.*, Database resources of the national center for biotechnology information. *Nucleic Acids Res.* **50**, D20–D26 (2022).
23. L. L. Moroz *et al.*, Neuronal transcriptome of *Aplysia*: Neuronal compartments and circuitry. *Cell* **127**, 1453–1467 (2006).
24. S. V. Puthanveettil *et al.*, A strategy to capture and characterize the synaptic transcriptome. *Proc. Natl. Acad. Sci. U.S.A.* **110**, 7464–7469 (2013).
25. Y. S. Lee *et al.*, Transcriptome analysis and identification of regulators for long-term plasticity in *Aplysia kurodai*. *Proc. Natl. Acad. Sci. U.S.A.* **105**, 18602–18607 (2008).
26. T. W. Abrams, W. S. Sossin, "Invertebrate genomics provide iInsights into the origin of synaptic transmission" in *The Oxford Handbook of Invertebrate Neurobiology*, J. H. Byrne, Ed. (Oxford University Press, 2019), chap. 4, pp. 123–149, 10.1093/oxfordhb/9780190456757.013.4.
27. E. Trinquet *et al.*, D-*myo*-inositol 1-phosphate as a surrogate of D-*myo*-inositol 1,4,5-tris phosphate to monitor G protein-coupled receptor activation. *Anal. Biochem.* **358**, 126–135 (2006).
28. S. Dutertre, N. G. Lumsden, P. F. Alewood, R. J. Lewis, Isolation and characterisation of conomap-Vt, a D-amino acid containing excitatory peptide from the venom of a vermivorous cone snail. *FEBS Lett.* **580**, 3860–3866 (2006).
29. F. M. Horodyski *et al.*, Isolation and functional characterization of an allatotropin receptor from *Manduca sexta*. *Insect Biochem. Mol. Biol.* **41**, 804–814 (2011).
30. E. Lismont *et al.*, Molecular cloning and characterization of the allatotropin precursor and receptor in the desert locust, *Schistocerca gregaria*. *Front. Neurosci.* **9**, 84 (2015).
31. H. Verlinden *et al.*, Characterisation of a functional allatotropin receptor in the bumblebee, *Bombus terrestris* (Hymenoptera, Apidae). *Gen. Comp. Endocrinol.* **193**, 193–200 (2013).
32. K. Vuerinckx, H. Verlinden, M. Lindemans, J. V. Broeck, R. Huybrechts, Characterization of an allatotropin-like peptide receptor in the red flour beetle, *Tribolium castaneum*. *Insect Biochem. Mol. Biol.* **41**, 815–822 (2011).
33. H. Verlinden *et al.*, The pleiotropic allatoregulatory neuropeptides and their receptors: A mini-review. *J. Insect Physiol.* **80**, 2–14 (2015).

34. G. Jékely, Global view of the evolution and diversity of metazoan neuropeptide signaling. *Proc. Natl. Acad. Sci. U.S.A.* **110**, 8702–8707 (2013).
35. O. Mirabeau, J. S. Joly, Molecular evolution of peptidergic signaling systems in bilaterians. *Proc. Natl. Acad. Sci. U.S.A.* **110**, E2028–E2037 (2013).
36. N. C. Dale, D. Hoyer, L. H. Jacobson, K. D. G. Pfleger, E. K. M. Johnstone, Orexin signaling: A complex, multifaceted process. *Front. Cell. Neurosci.* **16**, 812359 (2022).
37. S. D. Robinson *et al.*, Hormone-like peptides in the venoms of marine cone snails. *Gen. Comp. Endocrinol.* **244**, 11–18 (2017).
38. A. H. Jin *et al.*, Transcriptome and proteome of *Conus planorbis* identify the nicotinic receptors as primary target for the defensive venom. *Proteomics* **15**, 4030–4040 (2015).
39. T. Kenakin, A. Christopoulos, Signalling bias in new drug discovery: Detection, quantification and therapeutic impact. *Nat. Rev. Drug Discov.* **12**, 205–216 (2013).
40. T. Kenakin, C. Watson, V. Muniz-Medina, A. Christopoulos, S. Novick, A simple method for quantifying functional selectivity and agonist bias. *ACS Chem. Neurosci.* **3**, 193–203 (2012).
41. D. Wootten, A. Christopoulos, M. Marti-Solano, M. M. Babu, P. M. Sexton, Mechanisms of signalling and biased agonism in G protein-coupled receptors. *Nat. Rev. Mol. Cell Biol.* **19**, 638–653 (2018).
42. C. R. Squire *et al.*, Leucine aminopeptidase-like activity in *Aplysia* hemolymph rapidly degrades biologically active alpha-bag cell peptide fragments. *J. Biol. Chem.* **266**, 22355–22363 (1991).
43. W. Bawab, E. Querido, P. Crine, L. DesGroseillers, Identification and characterization of aminopeptidases from *Aplysia californica*. *Biochem. J.* **286**, 967–975 (1992).
44. B. S. Rothman *et al.*, *Aplysia* peptide neurotransmitters b-bag cell peptide, Phe-Met-Arg-Phe-amide, and small cardioexcitatory peptide B are rapidly degraded by a leucine aminopeptidase-like activity in hemolymph. *J. Biol. Chem.* **267**, 25135–25140 (1992).
45. L. Wickham, J. P. Zappulla, L. DesGroseillers, Molecular cloning, sequence analysis and expression distribution of an aminopeptidase in *Aplysia california*. *Comp. Biochem. Physiol. B Biochem. Mol. Biol.* **124**, 429–437 (1999).
46. S. D. Heck *et al.*, Posttranslational amino acid epimerization: Enzyme-catalyzed isomerization of amino acid residues in peptide chains. *Proc. Natl. Acad. Sci. U.S.A.* **93**, 4036–4039 (1996).
47. V. Gehmayr, C. Mollay, L. Reith, N. Muller, A. Jilek, Tight binding of transition-state analogues to a peptidyl-aminoacyl-L/D-isomerase from frog skin. *Chembiochem*. **12**, 1996–2000 (2011).
48. A. M. Torres *et al.*, D-amino acid residue in a defensin-like peptide from platypus venom: Effect on structure and chromatographic properties. *Biochem. J.* **391**, 215–220 (2005).
49. A. Jilek *et al.*, Biosynthesis of a D-amino acid in peptide linkage by an enzyme from frog skin secretions. *Proc. Natl. Acad. Sci. U.S.A.* **102**, 4235–4239 (2005).
50. Y. Shikata *et al.*, Isolation and characterization of a peptide isomerase from funnel web spider venom. *J. Biol. Chem.* **270**, 16719–16723 (1995).
51. M. S. R. Abid, S. Mousavi, J. W. Checco, Identifying receptors for neuropeptides and peptide hormones: Challenges and recent progress. *ACS Chem. Biol.* **16**, 251–263 (2021).
52. L. D. Fricker, L. A. Devi, Orphan neuropeptides and receptors: Novel therapeutic targets. *Pharmacol. Ther.* **185**, 26–33 (2018).
53. S. R. Foster *et al.*, Discovery of human signaling systems: Pairing peptides to G protein-coupled receptors. *Cell* **179**, 895–908 (2019).
54. A. Shiraishi *et al.*, Repertoires of G protein-coupled receptors for *Ciona*-specific neuropeptides. *Proc. Natl. Acad. Sci. U.S.A.* **116**, 7847–7856 (2019).
55. I. Gomes *et al.*, GPR171 is a hypothalamic G protein-coupled receptor for BigLEN, a neuropeptide involved in feeding. *Proc. Natl. Acad. Sci. U.S.A.* **110**, 16211–16216 (2013).
56. I. Gomes *et al.*, Identification of GPR83 as the receptor for the neuroendocrine peptide PEN. *Sci. Signal.* **9**, ra43 (2016).
57. A. P. Frei *et al.*, Direct identification of ligand-receptor interactions on living cells and tissues. *Nat. Biotechnol.* **30**, 997–1001 (2012).
58. N. Sobotzki *et al.*, HATRIC-based identification of receptors for orphan ligands. *Nat. Commun.* **9**, 1519 (2018).
59. B. M. Yussif, J. W. Checco, Evaluation of endogenous peptide stereochemistry using liquid chromatography-mass spectrometry-based spiking experiments. *Methods Enzymol.* **663**, 205–234 (2022).
60. S. Sharma, J. W. Checco, Evaluating functional ligand-GPCR interactions in cell-based assays. *Methods Cell Biol.* **166**, 15–42 (2021).